Zeitschrift: Helvetica Physica Acta

Band: 61 (1988)

Heft: 4

Artikel: On the optical properties of small metallic spheres

Autor: Giovannini, B. / Saniz, R.

DOI: https://doi.org/10.5169/seals-115961

Helvetica Physica Acta, Vol. 61 (1988) 566–571
0018–0238/88/040566–06$1.50 + 0.20/0

On the optical properties of small metallic spheres

By B. Giovannini and R. Saniz

Ecole de Physique de l'Université de Genève, Département de la Matière Condensée, 24, Quai E.-Ansermet, 1211 Genève 4-Switzerland

(8. V. 1988)

In honor of Martin Peter's 60th birthday.

Abstract. We calculate the photoemission spectrum for a small metallic sphere within the hydrodynamic approximation. For a diffuse surface this model predicts – besides the classical Mie resonance – additional resonances below the bulk plasma frequency, which depend on the equilibrium electron density profile and the depth of the surface region. These resonances are due to higher resonant Mie modes which do not exist for a sphere with a sharp surface. This model would explain observed resonances in the light-scattering intensity spectrum of small sodium particles.

1. Introduction

There has been much interest, in the past years, in improving the theoretical description of small metallic particles [1–3] because of a certain number of anomalous phenomena experimentally observed in these systems [4–6]. A better understanding of their optical properties will certainly give a deeper insight in all these phenomena. Here we focus on the photoemission spectrum. We consider a small 'jellium' sphere and describe the bounded electron gas within the hydrodynamic [7] approximation. This approximation has been considered earlier to study this problem [3, 8], but in our model we take into account the fact that the equilibrium electron density, n_0, is not discontinuous at the surface, but varies continuously from zero to the bulk value over some distance r_o. We calculate the absorption density according to the expression derived from the energy theorem by Forstmann et al. [9], and we integrate it over the sphere as a measure of the photoemission intensity. To solve the equations we use the multi-layer method, which we showed, in the case of a flat surface [10], to be equivalent to numerical integration.

2. The model

The basic equations are the retarded Maxwell's equations for a nonmagnetic material ($\mu = 1$) and the hydrodynamic equation. We recall the latter equation can be written

$$\frac{\partial}{\partial t}\mathbf{j} = \frac{\omega_p^2}{4\pi}\mathbf{E} - \gamma\mathbf{j} - \beta^2\nabla\rho, \tag{1}$$

where ω_p is the plasma frequency, γ is the damping factor and β the sound velocity. All these latter quantities are space dependent through n_o. Coupling all these the equations we find (after Fourier transforming in time), with $k = \omega/c$,

$$\nabla\times\nabla\times\mathbf{E} - \epsilon k^2\mathbf{E} - k^2(1-\epsilon)\frac{\beta^2}{\omega_p^2}\nabla(\nabla\cdot\mathbf{E}), \tag{2}$$

where $\epsilon = 1 - \omega_p^2/(\omega^2 + i\omega\gamma)$. For n_o constant the solutions of this equation are given by transverse and longitudinal spherical waves with wave vectors given by, respectively,

$$\begin{aligned} k_t^2 &= \epsilon k^2, \\ k_l^2 &= \frac{\omega_p^2}{\beta^2}\left(\frac{\epsilon}{1-\epsilon}\right). \end{aligned} \tag{3}$$

We divide the surface region in N layers$-N$ large$-$of thickness r_o/N and we take the unperturbed electronic density as constant in each one of them. Then in each layer the fields are given by the solutions with constant n_o, with the corresponding local density. We consider the development of these fields in spherical vector harmonics. Following the standard notation of Stratton [11], we have in the jth layer (we don't write the time dependence factor $\exp(i\omega t)$).

$$\begin{aligned} \mathbf{E}_{t\nu}^j &= \sum_{n=1}^{\infty} i^n \frac{2n+1}{n(n+1)}[a_{\nu n}^j \mathbf{m}_{o1n}^{\nu} - ib_{\nu n}^j \mathbf{n}_{e1n}^{\nu}], \\ \mathbf{H}_{\nu}^j &= -\frac{k_t}{k}\sum_{n=1}^{\infty} i^n \frac{2n+1}{n(n+1)}[b_{\nu n}^j \mathbf{m}_{e1n}^{\nu} + ia_{\nu n}^j \mathbf{n}_{o1n}^{\nu}], \\ \mathbf{E}_{l\nu}^j &= \sum_{n=1}^{\infty} i^n \frac{2n+1}{n(n+1)}\cdot id_{\nu n}^i \mathbf{l}_{e1n}^{\nu}. \end{aligned} \tag{4}$$

The subscript ν can take the values τ and ρ. In the first case it is a transmitted wave and we have to take spherical Bessel functions in the harmonics' expressions; in the second case it is a reflected wave and we take the spherical Hankel functions. Outside the sphere (vacuum) we have an electromagnetic wave of frequency ω coming along the z-direction, and we develop it also in spherical vector harmonics. Now in this problem we consider spheres of radius $R \simeq 10 - 50$ Å, and impinging beams of frequency $\omega \sim \omega_p$. Then $kR \ll 1$, so that the fields in the sphere are given by the first term in the development (4). This is the dipolar or *Rayleigh* approximation. To obtain the amplitudes we set the boundary conditions as follows. At the metal-vacuum interface we take the continuity of $\mathbf{E}_{\parallel}$, $\mathbf{H}_{\parallel}$ and $\mathbf{E}_{\perp}$. At the interface between two layers we need one more condition which we take as the continuity of $\beta^2\rho/\omega_p^2$ [9].

We introduce the following notation. At the nth layer, given by the interval $[r_{n-1}, r_n]$, we write the fields' wave vectors as k_t^n and k_l^n. Then we put

$$j_{nm}^{\sigma} \equiv j_1(k_{\sigma}^n r_m), \quad h_{nm}^{\sigma} \equiv h_1(k_{\sigma}^n r_m), \quad \sigma = t, l,$$

and introduce vectors $a_n = (a_{\tau 1}^n, a_{\rho 1}^n)$ and $b_n = (b_{\tau 1}^n, b_{\rho 1}^n, d_{\tau 1}^n, d_{\rho 1}^n)$. The continuity conditions at each boundary can now be expressed in matrix notation very simply by

$$\begin{aligned} \Gamma_{n,n} a_n &= \Gamma_{n+1,n} a_{n+1}, \\ \Lambda_{n,n} b_n &= \Lambda_{n+1,n} b_{n+1}, \end{aligned} \tag{5}$$

where the matrices Γ et Λ are given by

$$\Gamma_{n,m} = \begin{pmatrix} j_{nm}^t & h_{nm}^t \\ k_t^n j_{nm}^{t\prime} & k_t^n h_{nm}^{t\prime} \end{pmatrix}$$

and

$$\Lambda_{n,m} = \begin{pmatrix} \dfrac{j_{nm}^t}{k_t^n r_m} + j_{nm}^{t\prime} & \dfrac{h_{nm}^t}{k_t^n r_m} + h_{nm}^{t\prime} & -\dfrac{j_{nm}^l}{r_m} & -\dfrac{h_{nm}^l}{r_m} \\ k_t^n j_{nm}^t & k_t^n h_{nm}^t & 0 & 0 \\ \dfrac{j_{nm}^t}{k_t^n r_m} & \dfrac{h_{nm}^t}{k_t^n r_m} & -\dfrac{k_l^n}{2} j_{nm}^{l\prime} & -\dfrac{k_l^n}{2} h_{nm}^{l\prime} \\ 0 & 0 & (k_l^n)^2 j_{nm}^l & (k_l^n)^2 h_{nm}^l \end{pmatrix}.$$

In this way we have the n-th amplitudes in terms of the preceeding ones. Iterating this procedure we arrive to a system of equations in terms of the vacuum and bulk amplitudes. With the solution of this system we can easily calculate the amplitudes in all the layers iterating the procedure backwards.

3. Results

The electron gas parameters (bulk values) we use in our calculations are $\omega_p = 10^{16}\,\mathrm{s}^{-1}$, $\beta = 10^8\,\mathrm{cm}\cdot\mathrm{s}^{-1}$ and $\gamma = 0.03\,\omega_p$. These correspond roughly to those of sodium. The photoemission intensity, as we said in the introduction, is given by

$$A(\omega) = 4\pi \int_{\text{sphere}} d^3 r \frac{\gamma}{\omega_p^2} |\mathbf{j}|^2. \tag{6}$$

The main features of our results are the following:

(i) For a density n_o given by a 'step' function at the surface the spectrum shows a blue shifted Mie mode $(\omega_p/\sqrt{3})$. The oscillations above the plasma frequency are due to the longitudinal plasmon modes of the sphere. Ruppin [12] first found these modes using Lindhard dielectric functions in his calculations of extinction cross sections. Their influence is also clearly seen in the work of Doniach [8], who uses the field intensities in the z-direction at the surface to estimate the photoemission strength. The blue shift in the Mie mode was also stressed by Ruppin.

(ii) The most important feature of the non-constant n_o results is the appearance of higher *Mie modes* below the plasma frequency. Their dependence on the electronic density profile is twofold. In first place the intensity of these modes is higher when the derivative of n_o at the surface is lower. The reason is that these are electric type modes (like the classical Mie mode), due to transverse fields, and in the low density tail the dielectric function approaches unity, so that transverse fields move almost freely in this region. We can see this very clearly if we compare Figs. 1 and 2. On the other hand, longitudinal modes are strongly damped. The reason is again the low density at the surface, because the longitudinal wave vector tends to infinity, and for *spherical* waves this always means severe damping. We conclude, therefore, that a diffuse surface favors tranverse modes against longitudinal ones. (In fact there are also longitudinal modes below ω_p, but their influence is negligible as we just explained).

In second place the number of these modes depends on the diffuseness of the surface, r_o, i.e. for larger r_o more modes appear. We illustrate this in Fig. 3. We may add here that the photoeffect resonances are stronger for a smaller sphere radius (this is also true for a sharp surface).

(iii) In Fig. 1. the principal Mie mode is located at $\Omega = \omega/\omega_p = 0.55$, which

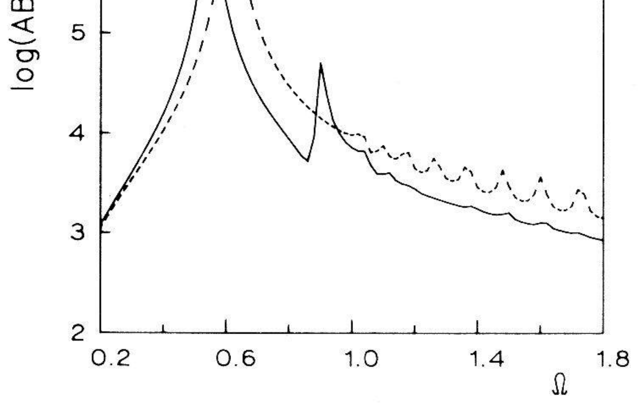

Figure 1
Absorption curve of a sphere of radius $R = 20$ Å with a linear density profile and surface diffuseness $r_o = 4$ Å. The broken curve gives the sharp surface results for comparison. Absorption is in arbitary units and $\Omega = \omega/\omega_p$.

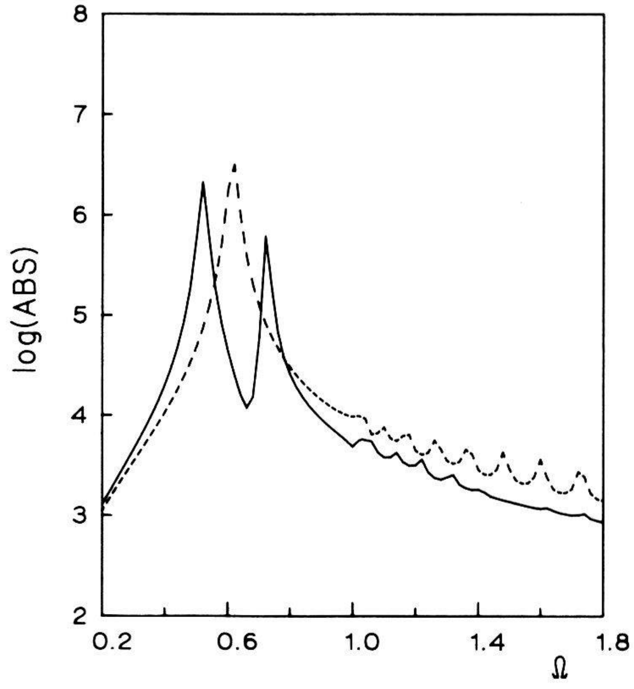

Figure 2
Same as Fig. 1 but with a $\sin^2(r\pi/2r_o)$ density profile to simulate a more realistic surface. We see that the second mode is much stronger.

means that now it is red shifted. It corresponds to a wavelength $\lambda \simeq 343$ nm for the plasma frequency we use. The secondary mode is at $\Omega = 0.9$, which corresponds to a wavelength $\lambda \simeq 209$ nm. In Fig. 4 we give the frequency-radius dipersion relation of these resonances. If we consider now the experimental results of Duthler et al [4], we see that we could qualitatively explain the second

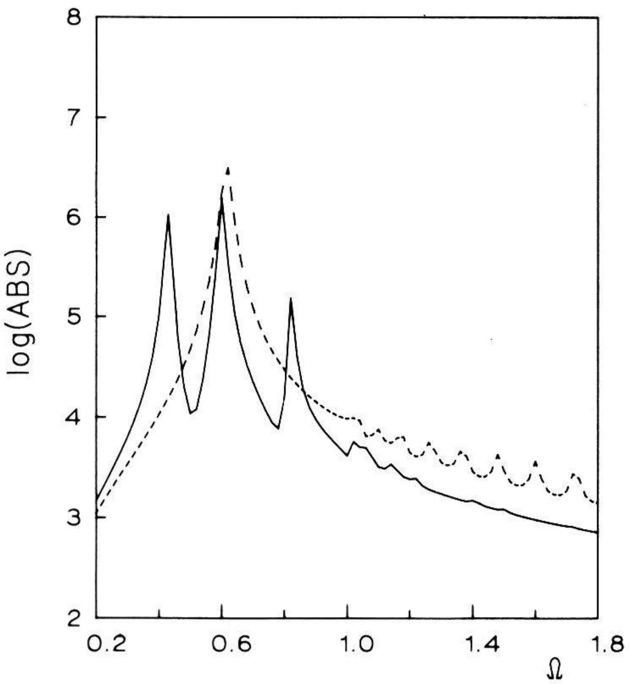

Figure 3
Same as Fig. 2, but with the diffuseness parameter set to 6 Å. This gives rise to a third Mie mode.

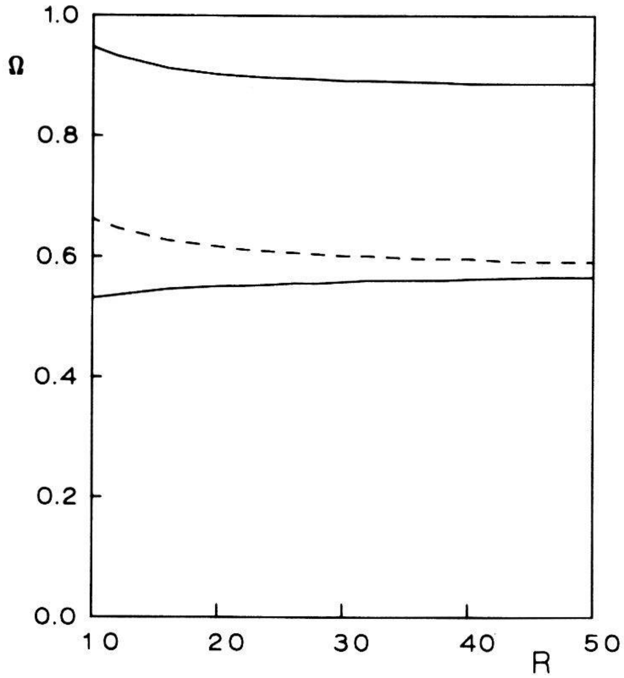

Figure 4
Frequency-radius dispersion relations of the Mie modes for a linear density profile and surface diffuseness $r_o = 4$ Å. The lower continuous line corresponds to the modified Mie mode and the upper one to secondary Mie mode. R (radius) is given in Angströms and $\Omega = \omega/\omega_p$.

maximum they observe as a resonance due to a secondary Mie mode -rather than a longitudinal mode as suggested by Ruppin [13]-induced by surface diffuseness. The exact location of the resonances will depend on the equilibrium electron density and the electron gas parameters one uses, but at this point more experimental data would be necessary before going further into quantitative considerations.

RERERENCES

[1] There are various interesting articles on this topic in *Electromagnetic Surface Modes*, A. D. Boardman ed., (John Wiley & Sons, 1982).
[2] G. Mukhopadhyay and S. Lundqvist, Solid State Comm. *44*, 1379 (1982).
[3] G. C. Aers and J. E. Inglesfield, J. Phys. F: Met. Phys. *13*, 1743 (1983).
[4] C. J. Duthler, S. E. Johnson and H. P. Broida, Phys. Rev. Lett. *26*, 1236 (1971).
[5] A. Schmidt-Ott, P. Schurtenberger and H. C. Siegmann, Phys. Rev. Lett. *45*, 1284 (1980).
[6] H. Burtscher and A. Schmidt-Ott, Phys. Rev. Lett. *48*, 1734 (1982).
[7] See, for example, F. Forstmann and R. R. Gerhardts, *Springer Tracts in Modern Physics*, vol. *109* (1986) or the article of A. D. Boardman in ref. [1].
[8] S. Doniach, *preprint*, Stanford University (1983).
[9] F. Forstmann and H. Stenschke, Phys. Rev. Lett. *38*, 1365 (1977).
[10] B. Giovannini and R. Saniz, Solid State Comm. *62*, 249 (1987).
[11] J. A. Stratton, *Electromagnetic Theory* (McGraw-Hill, New York, 1941).
[12] R. Ruppin, Phys. Rev. *11*, 2871 (1975).
[13] See the article of R. Ruppin in ref. [1], p. 384.